

Tribological behavior of a polymer grafted on silanized silica probed with a nanotip

T. Bouhacina, J. P. Aimé,* S. Gauthier, and D. Michel

CPMOH, Université Bordeaux I, 351 Cours de la Libération, F-33405 Talence Cedex, France

V. Heroguez

LCPO-ENSCP, Université Bordeaux I, Avenue Pey Berland, BP108, F-33405 Talence Cedex, France

(Received 27 February 1997)

The frictional forces between grafted layers on silica and a nanotip have been investigated as a function of the tip velocity. A comparative study has been performed between the friction behavior of the triethoxysilane molecules and polymer grafted on the silica. The polymer, a substituted polyacetylene, has been grafted following a two-step process. The silica surface is first pretreated with the triethoxysilane molecules, then the polymer is grafted on the silane molecules acting as a coupling agent. This two-step process allows the polymer to be firmly fixed. The good reproducibility of the data is accompanied by a robustness in the friction behavior. Both the silane molecules and the polymer grafted on the coupling agent show a linear increase of the force of friction with the logarithm of the sliding velocity. For the polymer, the force of friction is doubled that measured for the silane molecules and the forces of friction are found to be linearly dependent of the effective applied load. These two results are also supported by the measurement of the dynamic friction coefficient of the two grafted layers. The trends in these friction data have been found to be amenable to an analysis based upon a simple stress-modified thermally-activated Eyring model. A good consistency of the evolution of the different parameters, shear strengths, and barrier heights, computed with the model is obtained. From these results and their interpretation one gets a step forward for more quantitative information to be extracted with an atomic force microscope. Also, with the help of the Eyring model we provide a qualitative interpretation of what process is taking place to explain the increase of dissipation when the sliding experiment is performed on the grafted polymer. [S0163-1829(97)06435-7]

I. INTRODUCTION

Scanning probe microscopy (SPM) has evolved during the last decade to probe surface properties at the nanometer scale. Among them, scanning force microscopy (SFM) has shown a tremendous development, a part of which being dedicated to the study of tribological properties. For most of the engineers and scientists working in the field of tribology, friction force microscope (FFM) and more generally SFM are additional tools which give the possibility of probing friction processes at the nanometer scale, thus providing the opportunity of increasing the knowledge about friction.^{1,2}

Pioneering works were performed by Overney *et al.* and Radmacher *et al.* in which it was shown that organic films either physically or chemically adsorbed on the solid surfaces can exhibit a high friction contrast.^{3,4}

The description of energy dissipation during the friction process is still an unsolved problem. One reason is that one cannot access what is taking place at the interface during sliding, thus making quantitative analysis and interpretation difficult to achieve. When a nanotip is used, the situation is even worse as we do not have access to the contact area between the tip and sample, normally a rather large drawback as far as tribology is concerned.

Nevertheless, there are ways to overcome this main difficulty, either because an accurate knowledge of the contact area between the tip and sample is not required or because a comparison between several kinds of measurements on different samples allows the experimentalist to extract the relevant variations. One approach that has made progress in

removing some uncertainty at the tip-sample interface is increased control over the chemical nature of the two interacting surface species.^{5,6} Another tact that minimizes the absence of knowledge on the contact area is to investigate the influence of the tip velocity on the tribological behavior of grafted surfaces.^{7,8}

To get a better understanding of what is occurring under the tip, several attempts were performed, among which is the mechanical contact between two elastic solids.⁹⁻¹¹ Using such a theoretical framework means that the tip and volume of the sample under the tip are considered as continuum elastic medium. But up to now, there has been no clear experimental evidence that these theories can be called up to interpret most of the situations encountered with an atomic force microscope (AFM). Dissipation and plastic deformation may also occur, which, in many cases, make those theories less useful.

Some interesting attempts were performed in an ultrahigh-vacuum (UHV) AFM. Carpick *et al.*¹² have shown that the interfacial shear properties between the tip and surface was satisfactorily described with the help of the Johnson-Kendall-Roberts (JKR) model.¹⁰ But first it concerns a very specific experiment on fresh mica cleaved in UHV, and second, the radius of the tip was measured and found to be around 150 nm,¹² such that the curvature is rather smooth and cannot be considered as being truly on the nanometer scale. Putman *et al.*¹³ compare experiments performed in UHV and in air. The authors show that a linear relationship between the friction force and an effective load is obtained in UHV, while a JKR relation is obtained in air.

Putman *et al.* ended with the conclusion that a multisasperity effect occurs in UHV, while in air the influence of contaminant molecules induces a smooth contact.

Other attempts to understand the friction process was to evidence a clear relationship between the pull-off force, related to the adhesion, and the friction force. Using an AFM with tips coated with several different chemical species, Frisbie *et al.*⁵ show that the friction force increases as the pull-off force increases. The experiments performed with a scanning force apparatus (SFA) on various monolayers leads to a more subtle relation between adhesion and friction. The experimental results obtained by Yoshisawa *et al.*¹⁴ have been interpreted in a way indicating that the magnitude of the friction is proportional to the hysteresis of the adhesion rather than to the adhesion itself.

It does appear now that the relationship between the pull-off force and the friction is often verified experimentally with an AFM. Nevertheless, except for the work of Carpick *et al.*,¹² an exact, accurate demonstration of the use of the JKR model to describe friction measurements remains questionable.

A way to get a better understanding of the friction is to vary the velocity of the slider. This has been made in several experiments,^{7,8,14-19} showing its influence and becomes to be more regularly used with an AFM. The effect of the sliding velocity can be of some help to access to the structure of the investigated monolayers. As suggested with the dynamic phase diagram representation of the rate of energy dissipation as a function of the sliding velocity,^{14,15,17,18} we can decide either if the monolayer has a liquid, solid, or amorphous structure. Typically in the range of velocity accessible with the AFM (micrometer per second), one cannot expect to observe any velocity dependence if the monolayer is too much rigid or compact. Only when a liquid state is met do we expect to measure an effect.

Beyond a dynamic phase diagram, several phenomenological models have been used to get more quantitative information. One is to borrow an approach describing the viscoelastic behavior of complex polymer materials such as the William-Landel-Ferry (WLF) approach.^{14,15,17,18} It has been discussed in a few occasions, but the structure of the equation is not very convenient as it does not give an easy tractable relationship between the velocity and friction force.^{7,20} Therefore, the main help is to give a way to fit data showing that the amount of energy dissipation is velocity dependent.

Another phenomenological model is an Eyring-type model of thermally activated process.^{21,22} Experimental works have been successfully described that way.¹⁵ Pressure, temperature, and velocity dependence of friction on Langmuir films were satisfactorily described using a thermally activated process. Experiments were performed with a SFA apparatus, therefore giving a contact area within the micrometer scale. The question arises that such a behavior can also be observed with a sharp AFM tip where a single asperity contact can be expected. Moreover, a recent molecular dynamics study has been done showing that the friction of monolayers involving a contact area of a few square nanometer can be accounted with the thermal activation model.²²

In a preceding study⁷ we have shown that the good reproducibility of the tip velocity dependence on the frictional force provides an interesting way to characterize the grafting

process with organosilane molecules. In the present paper we move a step forward by grafting a polymer on the silanized silica surface. Also, a phenomenological model is employed (Eyring model), allowing us to describe more accurately the different steps of the grafting process. In addition, the Eyring model provided a useful way to compare the present experimental results to friction data obtained on self-assembled monolayers at a macroscopic scale. The paper is organized as follows: In Sec. II are given the experimental conditions required to obtain reproducible friction data and the experimental results are presented; in a Sec. III the data are compared to the Eyring model, and Sec. IV is devoted to a discussion.

II. EXPERIMENTAL RESULTS

A. Experimental conditions

Except for the grafted polymers, sample preparation and experimental conditions are described in great details elsewhere.⁷ Here we only recall which do appear as the most important experimental constraints required to get robust, reproducible friction data with an AFM. The experiments have been performed with a Nanoscope III from Digital Instrument.²³

The experimental results presented in this work were obtained in a gloves box in which the ppm of O₂ and H₂O is achieved. This condition seems to be necessary since the few experiments we have performed in air were not reproducible enough to extract a significant variation of the friction as a function of the tip velocity.

The feedback loop was never used, because when one allowed the piezoactuator to move, erratic results were often obtained. Several qualitative explanations can be put forward to understand the difficulties in getting reliable data when the feedback loop was used. The feedback loop allows the piezoactuator to have a vertical motion, which is a requirement necessary to record an image of a surface at a more or less large scale. But this vertical motion produces an additional random noise rendering measurement more difficult to achieve when deflection of nanometer range must be accurately measured. Also, such a vertical motion induces an additional fluctuation of the contact area between the tip and sample, which in turn affects the measure of the force of friction. Therefore, uniquely, the deflection of the cantilever was measured, keeping the piezoactuator at rest with a null applied voltage throughout the experiments.

In Fig. 1 are sketched the different situations investigated. As described in Ref. 7, several organosilanes were studied that all show the same behavior as a function of the tip velocity. Here we shall focus the attention on the results obtained on the 3-ethoxysilane ended with a thiol group of formula HS-CH₂-Si(OEt)₃ and on the grafting of a polymer on the 3-ethoxysilane.

The polymer chosen is a substituted polyacetylene with substituent side groups ended with a chlorine atom of generic formula —HC=C(CH₂)₃Cl—_n. This polymer is fairly rigid²⁴ and can be assimilated to a rodlike object; the molecular weight is $M_w = 14\,700$, corresponding to a contour length of the backbone of 20 nm. The chemical reaction allowing the polymer to be grafted on the organosilane molecules is given by the reaction between the chlorine atom

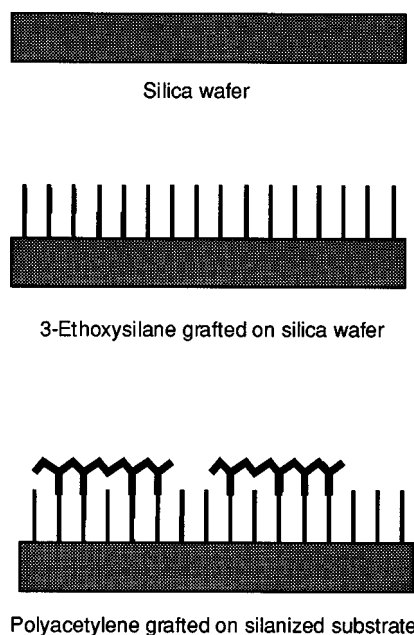


FIG. 1. Sketch of the surfaces investigated.

and the thiol group as described in Ref. 25. Therefore, the chain can be fixed at the coupling agent in several locations along the polymer backbone.

Three grafted silica surfaces with the organosilanes molecules and two samples with the grafted polymer were investigated. Four different tips and three cantilevers were used k_1 , k_2 , k_3^a , and k_3^b ; the announced stiffnesses are reported in Table I. The experiments and identical sample preparations were performed over 2 years and always give the same results. The measurements were done at zero externally applied load. Each time a grafted polymer sample was prepared, a new silica surface and a new silica surface grafted with 3-ethoxysilanes were also prepared.

TABLE I. Computed area of contact and interface shear strength with different stress activation volumes (see discussion in Sec. IV D). Q is the barrier height, Δ the additional vertical deflection of the cantilever due to the tangential force F_f . $F_f = k_t \Delta / 2$ and the pull-off force is given by $F_{PO} = k_v \Delta_p$, where Δ_p is the vertical piezodisplacement needed to unstuck the tip.

Probe	Sample	$\Phi = 0.2 \text{ nm}^3$		$\Phi = 5 \text{ nm}^3$		Q (10^{-20} J)	Δ (nm)	F_f (nN)	F_{PO} (nN)
		A (nm^2)	τ (5 $\mu\text{m/s}$) (MPa)	A (nm^2)	τ (5 $\mu\text{m/s}$) (MPa)				
k_2									
$k_v = 0.12 \text{ N/m}$	Silanized wafer	14	213	348	8.6	10.8	1.2 ± 0.3	6.1 ± 1.5	77 ± 1
$k_L = 5.1 \text{ N/m}$	Grafted polymer on Silanized wafer	12	419	298	16.9	14.4	2.0 ± 0.3	10.2 ± 1.5	72 ± 1
k_1									
$k_v = 0.58 \text{ N/m}$	Silanized wafer	85	284	2118	11.4	12	3.3 ± 0.3	48.8 ± 1.5	209 ± 6
$k_L = 14.8 \text{ N/m}$	Grafted polymer on Silanized wafer	76	574	1898	23	17.6	5.9 ± 0.3	82.9 ± 1.5	168 ± 5
$k_3^{(a)}$									
$k_v = 0.38 \text{ N/m}$	Silanized wafer	44	270	1088	11	11.8	2.5 ± 0.3	24.3 ± 1.5	125 ± 1
$k_L = 9.7 \text{ N/m}$	Grafted polymer on Silanized wafer	42	508	1041	20.5	16.3	4.4 ± 0.3	42.7 ± 1.5	108 ± 1
$k_3^{(b)}$									
$k_v = 0.38 \text{ N/m}$	Silanized wafer	376	110	9402	4.4	9.6	8.6 ± 0.3	83.4 ± 1.5	399 ± 1
$k_L = 9.7 \text{ N/m}$									

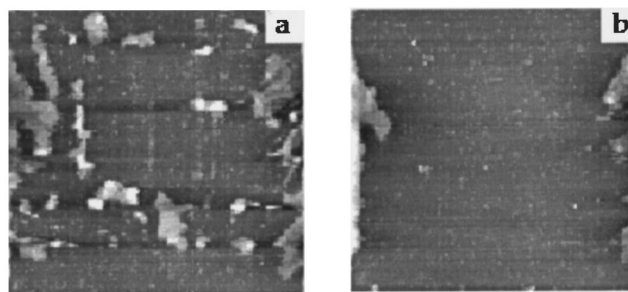


FIG. 2. Image $10 \mu\text{m} \times 10 \mu\text{m}$ of polyacetylene physisorbed on silica. (a) Image obtained after one scan. (b) The same location after several scans of the probe, the polymer is removed.

B. Experimental results

To check the efficiency of the coupling agent, the polymer was first deposited on the silica surface. Figure 2 shows the images obtained; the polymer is easily removed by the tip rubbing the surface. No more than one scan can move away the polymer adsorbed. On the contrary, when the coupling agent is used, whatever the number of scans recorded, the tip is unable to move the polymer and the images remain identical. The topography is markedly different from what has been obtained when uniquely the organosilane molecules were grafted (Fig. 3). Therefore, from a comparison between Figs. 2 and 3, we can conclude a success in grafting the polymer on the coupling agent and that the polymer is now firmly fixed at the surface.

A systematic study of the tribological properties of the grafted polymer was thus performed to better understand the structure of the layers. Figure 4 shows the experimental results obtained on the three samples, the silica, the organosilane, and the polymer. As previously discussed, the layers of organosilane molecules exhibit a characteristic velocity dependence which is not observed with the silica in the veloc-

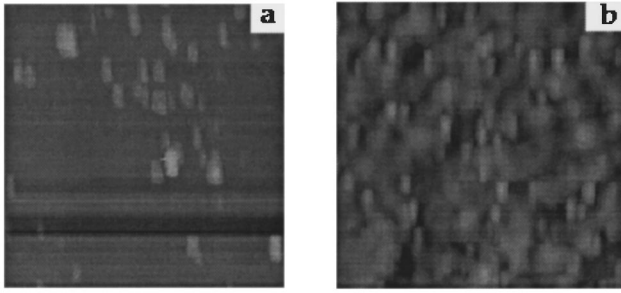


FIG. 3. (a) Image $1\ \mu\text{m}\times 1\ \mu\text{m}$ of 3-ethoxysilane grafted on silica. (b) Image $1\ \mu\text{m}\times 1\ \mu\text{m}$ of polyacetylene grafted on silanized silica. The surface remains identical after several scans.

ity domain investigated. Similar results were obtained when using the other probes (Fig. 5). For the polymer samples, also the same velocity dependence of the friction is observed (Fig. 6).

The magnitudes of the pull-off force measured on the polymer are slightly smaller than the ones measured on the organosilane layers. In spite of similar pull-off forces, when the polymer is grafted a further increase of a factor of 2 of the friction force is observed. Contrary to what is expected, the increase of the friction force is not followed to an increase of the pull-off force. This makes a difference with what was observed on the different organosilane molecules, for which higher pull-off forces were accompanied in most cases by higher friction forces. Therefore, for the polymer grafted on the coupling agent, the origin of the friction force is not simply related to adhesive forces.

As shown in Fig. 6, the rate of energy dissipation is larger for the polymer grafted on organosilane, but the slopes are nearly identical. This result suggests a very similar behavior for the two organic films, but with a force of friction twice as large for the polymer.

In Fig. 7 is reported the variation of the force of friction as a function of the externally applied load. The friction coefficients deduced from the slope are velocity dependent for

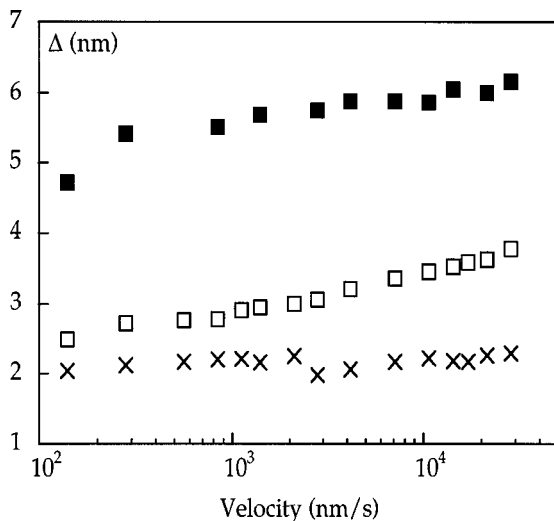


FIG. 4. Friction versus tip velocity, at zero externally applied load, with the cantilever k_1 on the three samples: silica (crosses), organosilanes grafted on silica (open square), and polymer grafted on organosilanes (solid square).

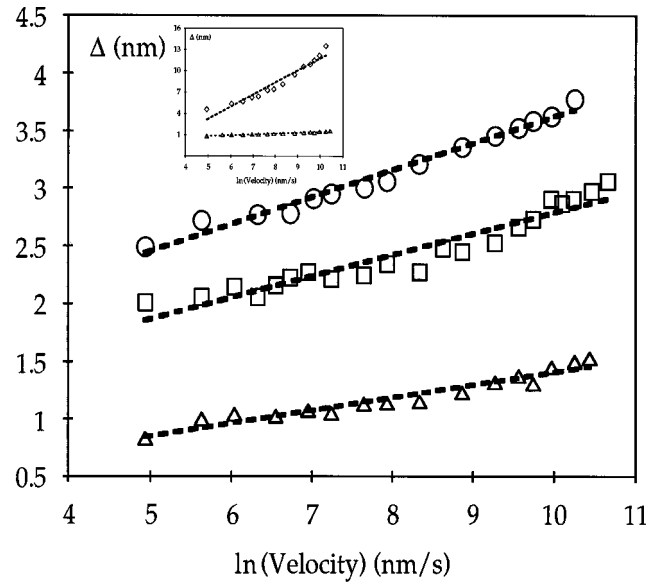


FIG. 5. Fits and experimental data of friction versus tip velocity for the organosilanes grafted on silica and probed with three cantilevers: k_2 (triangle), k_1 (square), and k_3^a (circle). Fits are obtained with the use of Eq. (5). The results of the fits are given in Table I. In the inset are reported the experimental data obtained with the probe k_3^b (lozenge).

the organic films, so that the slopes give the two dynamical coefficients of friction, $\mu(V)$. The friction coefficient of the silane molecules is closed to that of the silica, while $\mu(V)$ is twice as large for the grafted polymers. This result is in complete agreement with the observed velocity dependence of the two layers.

III. MODELING THE INFLUENCE OF THE SLIDING VELOCITY

A first analysis restricted to the silanes experimental results was given in Ref. 7. As shown in this paper, the use of the WLF equation gives good fits, but is unable to extract information to interpret the friction data.

Here we shall interpret the overall results including the ones obtained on polymer PA through the use of a Eyring-type model of thermally activated process. The Eyring model has been adapted to describe the plasticity of solid and account for the motion of dislocations in vitreous polymer.²⁶ Also, it provides a phenomenological model for the viscosity in liquids. This model has been extended to interpret dissipation processes in sliding experiments.^{15,27}

The interface between the slider and sample is characterized by a shear strength which may become a function of the temperature, pressure, and velocity. The relationship between the shear stress τ , the contact area A , and the measured force of friction F_f is given by

$$F_f = \tau A. \quad (1)$$

In a thermally activated process under a shear stress, a flow of particles can take place from which one has to calculate an average velocity (Fig. 7). For a particle in an harmonic potential of barrier height Q , the probability of occupation at a specific location is given by the product of the

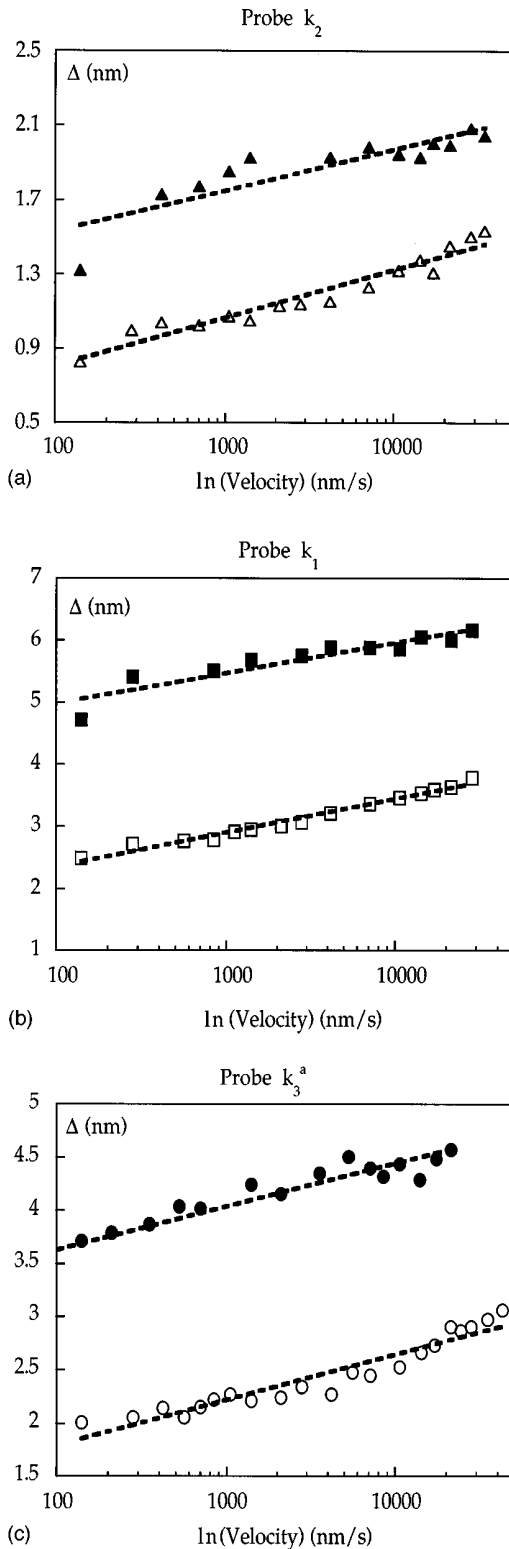


FIG. 6. Semilogarithms of fits and experimental data of friction versus tip velocity for the organosilanes grafted on silica and polymer grafted on the silanized substrate with (a) the cantilever k_2 , (b) the cantilever k_1 , and (c) the cantilever k_3^a .

vibration frequency of the particle or mobile molecule and the Boltzmann factor. The probabilities of jumping to the left or to the right are equal, leading to a null average velocity.

If we consider a one-dimensional periodic distribution of barriers of spatial period b , under shear force the potential

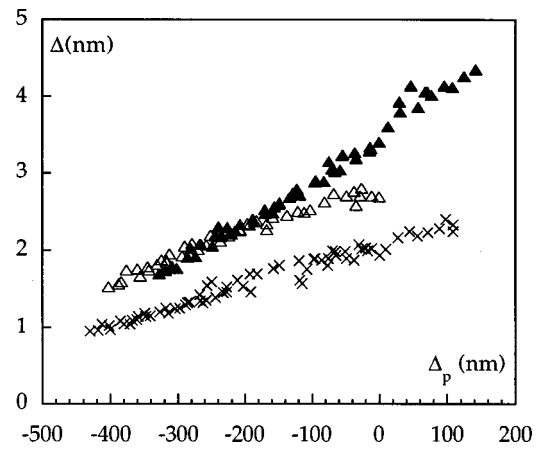


FIG. 7. Frictional force versus vertical piezoelectric displacement (cantilever k_2 is used). For convenience, a zero value corresponds to a null externally applied load, that is, an effective applied load equal to the pull-off force F_{PO} . Silica surface (crosses) $0.05 \leq \mu \leq 0.07$, organosilane (open square) $0.06 \leq \mu \leq 0.08$, and polymer (solid square) $0.11 \leq \mu \leq 0.15$.

barriers are distorted and the average velocity v is given by

$$v = 2\nu b \exp\left[-\frac{Q}{kT}\right] \sinh\left(\frac{\tau\phi}{kT}\right), \quad (2)$$

where ν is the vibrating frequency of the molecule in the unperturbed harmonic potential, τ the shear strength of the slider-monomer interface, and ϕ is referred as the stress activation volume. The barrier height Q is governed by the repulsive interaction between neighboring molecule units (see Fig. 8).

If the force and temperature are small enough, the molecule is restricted to small motions inside the harmonic potential with a relaxation time given by ν . A typical frequency of molecule units of 1 nm length or less is 10^{11} Hz, which gives for a period $b=0.5$ nm a velocity $v_0=100$ m/s. For such an excitation, the energy dissipation occurs through phonons. Such a process leads to abrupt changes in the friction signal in which short relaxation times are involved corresponding to a stick-slip behavior.

At higher temperatures and higher shear forces, a continuous energy dissipation similar to that of liquid viscosity can occur. In that case, characteristic times are much longer and the friction increases sublinearly with the velocity. Depending on the barrier height, the phenomenological equation (2) predicts that measure of the friction can exhibit such a behavior in the $\mu\text{m/s}$ range, a domain of velocity accessible with an AFM.

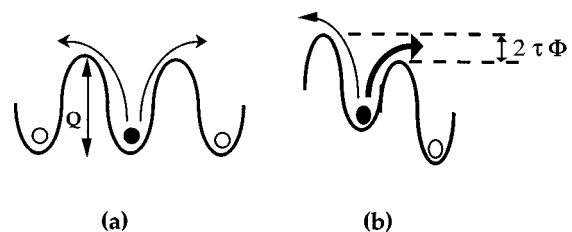


FIG. 8. Sketch of a double-well potential distorted by an external shear force.

In the sliding experiments we do not observe the velocity v of the rate-controlling process, but the sliding velocity V of the nanotip. With the assumption that v is simply proportional to the velocity of the nanotip $V = \alpha v$ and of the observed exponential dependence of velocity on shear stress (i.e., $\tau\phi > kT$), Eq. (2) becomes

$$V = V_0 \exp \left[- \left(\frac{Q}{kT} - \frac{F}{A} \frac{\phi}{kT} \right) \right], \quad (3)$$

where $V_0 = \alpha v b$ and Eq. (1) has been used. Equation (3) can be rewritten such that the relationship between the additional vertical cantilever deflection Δ due to the friction force and the velocity appears explicitly:

$$F_f = k_t \frac{\Delta}{2}, \quad (4)$$

where k_t is the cantilever stiffness that gives the vertical deflection connected to the tangential force in the plan of contact between the tip and the sample. k_t is simply related to the announced cantilever stiffness and the geometrical parameters of the lever.^{4,27,28} The phenomenological equation compared to the experimental results is given by

$$\Delta = \frac{2A}{k_t \phi} kT \ln \left(\frac{V}{V_0} \right) + \frac{2A}{k_t \phi} Q. \quad (5)$$

At room temperature, $kT \sim 4.1 \times 10^{-21}$ J and k_t can be estimated (see Table I).

There remain four unknown parameters: the velocity V_0 , the area of contact A , the barrier height Q , and the stress activation volume ϕ . As shown with the fit performed by Briscoe and Evans¹⁵ (paragraph IV-4), a variation of one or two orders of magnitude of V_0 does not change the general trends, so that using a value of $V_0 = 100$ m/s is a reasonable assumption. For the stress activation volume, it is a more complicated matter. The exact physical meaning of ϕ is less clear. Let us consider first that it is related to the volume of a molecular unit so that $\phi \sim 0.2$ nm³. With the help of these assumptions, the fit of the experimental data points gives the two other parameters A and Q . The results are reported in Table I.

In spite of the wide range of contact area calculated with the help of Eq. (5) and even considering that the geometry of the contact area between the tip and layer can vary significantly, the quantities of interest which are related to the dissipation process remain remarkably close. Except for the tip k_3^b the shear strength, which is obtained from the computed values of the contact area and equation (1), varies between 210 and 290 MPa, while the barrier height varies between 1 and 2×10^{-19} J. Even more interesting is the systematic difference between the shear strengths of the PA grafted on the organosilane molecules and the ones of the organosilane layers themselves. The shear strengths are systematically a factor of 2 higher when the polymers are measured, while the ratio of the effective barrier heights shows also a remarkable stable value with values ranging between 1.3 and 1.45.

IV. DISCUSSION

A. Preliminary remarks

Before attempting to extract more quantitative information, it is worth discussing first some technical and experimental points. Except when friction data are recorded as a function of the externally applied load (paragraph IV-2), an additional well-known difficulty encountered when using an AFM is that we do not accurately know the stiffness of the cantilever k_v .^{30,31}

The stiffness of the cantilever follows a cubic law as a function of the thickness.^{9,32} As the thickness is below the micrometer, the cubic law and this small thickness explain the reason why one can get scattered values of the stiffness.

The lateral stiffness used in this work scales as $k_t \sim (L/h)k_v$, where L and h are the length of the cantilever and the height of the tip, respectively. Therefore, additional uncertainties due to the geometrical factor of the cantilever-tip system are negligible since the dependence is linear and that significant relative errors on the length and the tip height are not expected because of their much larger values, more than 100 and a few micrometers, respectively.

If we do consider that the announced stiffnesses are the correct ones, at first sight, there are magnitudes of the friction forces which do not seem to match the cantilever stiffnesses. For example, let consider the two extreme cases represented by the experimental results obtained with the k_3^b and k_2 . The calculated vertical stiffnesses give a factor of 2, while the friction measured at a velocity $v = 5$ μ m/s with the k_3^b is a factor of 7 higher than the one measured with the k_2 . Also, the pull-off force measured with the k_3^b is a factor of 5 larger than the one measured with the k_2 , and therefore again a different value is obtained, still not reaching the one deduced from the friction measurement.

From the Deryaguin approximation or the JKR model,^{10,33} we derive that the adhesive force is proportional to the radius of curvature of the tip:

$$F_{PO} = F_{adh} = CWR, \quad (6)$$

where W is the Dupré work of adhesion and, in these experiments, the constant C can be assumed as being the same whatever the cantilever used.³¹

Taking the smallest pull-off force as a reference, we obtain a relative evolution of the ratio between the pull-off forces, which in turn give the relative evolution of the radius of curvature of the four different tips (Table II). When these values are compared to the ones obtained from the computed area A , one gets an excellent agreement and the apparent discrepancy disappears. Both the fits of the friction data points and the measurements of the pull-off force indicate that the large differences are mostly due to a change of the size of the tip.

This result is completely sustained by the different measurements performed on the organosilane molecules and on the polymers. As a consequence, if one cannot access accurately quantitative stiffnesses, it remains that their relative values are certainly the good ones. Because of the very good consistency obtained and leaving aside that the force might not be quantitatively accurate, we conclude that our estima-

TABLE II. Ratios of the area of contact computed from the friction data and of the pull-off forces. The values used as reference are obtained with the cantilever k_2 . 3-ethoxysilane (a) and polymer grafted on silanized silica (b).

	(a)		
	$\left(\frac{A_{k_i}}{A_{k_2}}\right)$	$\left(\frac{F_{PO_{k_i}}}{F_{PO_{k_2}}}\right)^2$	$\left(\frac{F_{PO_{k_i}}}{F_{PO_{k_2}}}\right)^{4/3}$
k_1	6.1	7.4	3.8
k_3^a	3.1	2.7	1.9
k_3^b	26.9	26.9	9.0
	(b)		
	$\left(\frac{A_{k_i}}{A_{k_2}}\right)$	$\left(\frac{F_{PO_{k_i}}}{F_{PO_{k_2}}}\right)^2$	$\left(\frac{F_{PO_{k_i}}}{F_{PO_{k_2}}}\right)^{4/3}$
k_1	6.3	5.4	3.1
k_3^a	3.5	2.3	1.7

tion of the lateral stiffnesses does not introduce an additional uncertainty when using Eq. (5).

B. Relationship between adhesive and friction forces

Since the experiments were performed at null externally applied load, the pull-off force is a measure of the effective applied load. The JKR model predicts that the area of contact varies as

$$A \sim (F_{PO}R)^{2/3} \sim (WR^2)^{2/3} \sim R^{4/3}. \quad (7)$$

As expected from the preceding analysis, the relative evolutions of the ratios of the contact area calculated from the pull-off forces and expression (7) do not agree with the ones deduced from the friction data (Table II). For example, the two extreme cases give a factor of 9 between the two respective contact areas, that is, a factor of 3 times less than the one computed from the friction data.

For an elastic response of the organic films following the Hook law, the elastic displacement δ depends linearly of the effective applied load, that is, $\delta \sim F_{PO}$. For values of δ much smaller than the radius of the tip, a simple geometrical assumption gives the area of contact between the sphere and plane surface:

$$A \sim \delta R \sim WR^2, \quad (8)$$

which is the relationship obtained between the pull-off force measurements, with the use of the Eq. (6), and the areas of contact computed from Eq. (5) and the friction data (Table II).

Therefore, whatever the size of the tip we have used, these results indicate that a linear relationship holds between the effective applied load and the contact area between the tip and layer. Rather than a JKR model, the use of the Amontons' law is more suitable.

The whole picture is supported by the measurement of the friction as a function of the externally applied load. Polymers and silane molecules exhibit a linear behavior (Fig. 7). The comparison of the friction coefficients $\mu(V)$ give results in

very good agreement with the relative shear strengths calculated in Table I. The friction coefficient of the grafted polymer surface is 0.13, while the friction coefficient of the silane film is 0.06. The friction coefficient measured for the silica, which is velocity independent, is 0.06, a value smaller than the one previously obtained with an AFM.¹³ At $0.7 \mu\text{m s}^{-1}$, the silane film is almost equal to the silica one, a rather high friction coefficient,^{3,34} which indicates that the layer made of the triethoxysilanes does not act as a lubricant.

Here it is important to note that, when recording friction data as a function of the externally applied load, the way we measure the friction^{7,29} does not need to know the cantilever stiffness. The friction deflection is given by $\Delta/2 = \frac{3}{2}(h/L)\mu(V)\Delta_p$, where Δ_p is the vertical motion of the piezoactuator. Thus, if our calibration of the cantilever deflection is correctly done, which is very easy to perform, one gets a direct absolute measurement of the friction coefficient.

We have already noted that while the friction of the polymer is systematically higher of a factor of 2, the pull-off force is slightly smaller. The differences between the pull-off force are small, from 5% to 10%, but, since they have been systematically measured, are significant.

A friction force much larger when the pull-off forces are nearly identical does not fit the expected behavior. An increase of the friction as function of the pull-off force seems quite obvious since the magnitude of the friction increases as the contact area increases and therefore must do with the effective applied load. Nevertheless, a more subtle relation between adhesion and friction has been suggested by Yoshizawa *et al.*¹⁴ Their recent experimental work performed with a SFA apparatus shows that the friction force is more likely to be a function of the hysteresis of adhesion rather than being a direct function of the force of adhesion itself. In other words, the energy dissipation becomes the difference in energy between advancing and receding the contact area during the translation motion of the tip, a situation similar to what happens in a force curve when the tip is approached and then retracted from the sample. We do not have the sensitivity to measure accurately the shape of the instability of the microlever when the tip approaches the surface. Uniquely, the pull-off force, corresponding to the retraction, can be measured, so that we cannot perform a comparative study between friction and hysteresis of adhesion. As shown below, taking advantage of the changes observed between grafted polymers and silane molecules, we get a further insight into the origin of the increase of the friction without the need of an increase of the adhesive force.

C. Influence of the tip velocity on the force of friction

In their review article Overney *et al.* stress that AFM results of variable velocity cannot be explained by the Eyring model of friction, while it does as a function of the pressure.^{3,34} The main reason was that any velocity dependence was associated with wear of the layer. In their experiment, the smaller the tip velocity, the larger the friction, the increase of friction being accompanied by a noticeable damage of the film.

As we have shown in Ref. 7, we also have observed such a behavior in some circumstances and clear evidence that the increase of the friction force as the tip velocity decreases was

always connected to damage in the films. Note also that recent experiments performed at the macroscopic scale have shown a velocity weakening of the friction. This velocity weakening is interpreted by a creep process, the strength of which being increased with the age of contact between the slider and the surface.²⁷ This appears similar to the observed V weakening with an AFM, as it was systematically accompanied by evidence of plastic deformation or serious damage on the film.

When the behavior is of the Eyring type, as described in the present work, the layers remain remarkably stable. Each data point shown in the present work corresponds to an average of several measurements, and this means that to record a velocity dependence, the same surface location must be scanned several hundred times without showing any modifications. A similar V strengthening of the force of friction has been recently observed with an AFM, in which, also, no specific damage of the layers was reported.⁸

The main interest of the Eyring model is to provide information, barrier heights and shear strengths, which gives a fruitful comparison between the two series of measurements. As shown in Table I, the barrier heights are higher for the polymer, showing at least an increase of about 30%.

Glosli *et al.*²² in their molecular dynamic simulation express the barrier height as a function of an effective number of molecules involved in the friction process. The barrier height for one molecule is given by the repulsive strength between molecules and is set equal to $70k_B$. To describe the barrier height in terms of an effective number of molecular units is questionable, and, as underlined by the authors, there is no reason to expect that the barrier height can be simply connected to the area of contact.

Nevertheless, it can help to understand the increase of barrier height as being an increase of the number of molecules involved in the dissipation process. If so, our experimental data show that this number does not depend of the contact area (Table I). In spite of the wide range of contact areas and whatever the series of samples measured, silanes molecules or polymers, within the same series of layers we get values of the barrier height nearly identical. In other words, the force of friction is proportional to the number of molecules under the tip, the area of contact, but the number of molecules that characterizes the process to produce the dissipation of energy remains independent of the number of molecules involved in the contact.

As the stress activation volume, the exact physical meaning of the barrier height is difficult to access. The base line of a microscopic description of the viscous forces is that the transfer of moment occurs through motions bringing the molecules into contact. Following this framework and because of the simple chemical structure of the polymer, a qualitative interpretation can be drawn.

A chemical function has been synthesized at each monomer unit, allowing the polymer backbone to be grafted on several organosilane molecules. Moreover, because of the conjugated backbone, polyacetylene might have a more rigid structure than usual polymer with saturated covalent links.²⁴ Therefore, through the chemical links and the polymer backbone, a coherent motion of organosilane molecules can be induced. The number of monomer units per polymer is about 80, so that for an energy dissipation related to motion that

brings molecules into contact, the effective unit involved contains more molecules when the grafted polymers are involved. For each equivalent translation motion induced by the tip, the number of repulsive contacts increases, from which one can expect an increase of the barrier height.

When rubbing the grafted polymers, the interface shear strengths are found to be systematically the double of the ones measured on the silanes. But those results are obtained by keeping the stress activation volume identical for the two types of layers.

There is *a priori* no particular reason to use the same stress activation volume for the silane molecules and the polymer grafted on the connectors. The use of a stress activation volume twice as large for the polymer will give the same shear strength for the two series of samples. It will also give an area of contact twice as large for the polymer in spite of smaller pull-off forces. As shown in Table I, keeping the same stress activation volume provides a very good agreement between the relative pull-off forces and the contact area. The contact areas for the polymer samples computed from the friction data are systematically slightly smaller than the ones obtained for the silane layers, exactly as the pull-off forces behave. Therefore, to keep coherent the discussion of the results, we consider that the large increase of the friction is related to an increase of the shear strength, such a choice being completely sustained by the analysis given in Secs. IV A and IV B.

Following this aim, the same qualitative arguments can be used to understand the increase of the shear strength. Because of the rodlike structure of the polymer, the silane molecules are more tightly fixed; thus, the units are more rigid, leading to a structure with a higher spring constant, which in turn leads to a higher shear strength to move the unit at the same velocity.

D. Comparison with friction data obtained at larger scale on Langmuir films and rubbers

Because of the good robustness of the friction data and the coherent picture obtained when the Eyring model is used, it becomes interesting to compare in more details the AFM results to the ones obtained by Briscoe and Evans. For their experiments, the contact area is at the macroscopic scale, thus several orders of magnitude higher than the one we have with a nanotip. As a consequence, the authors have access to the contact area which allows them to reduce the number of unknown parameters. Therefore, the stress activation volume can be calculated instead of being set arbitrarily.

The main point is to evaluate the influence of V_0 , since in any sliding experiment what is measured is the slider velocity. Using several V_0 values between 7.7×10^{-2} and 1700 m s^{-1} , the authors found values of ϕ between 3 and 6.6 nm^3 . A direct consequence of the use of a large activated volume, for example, 5 nm^3 , corresponding to $V_0 \sim 20 \text{ m s}^{-1}$, is that the contact radius computed is between 10 and 25 nm, thus leading to a rather large area of contact between the tip and layer.

Using the procedure described in Ref. 35, we get an estimation of the radius of the tip. For example, we estimate for the k_2 a tip radius between 20 and 25 nm and for the k_3^a a tip radius between 50 and 60 nm. The k_3^b is clearly broken,

which can be straightforwardly deduced from the data reported in Table I. These measurements are indicative since the assumptions are based on a geometrical analysis.³⁴ Such an approach assumes a smooth, spherical shape, at the very end of the tip and thus cannot give the fine structure of the tip.

These values provide information suggesting that the radius of the contact area is about the one of the tip, which is unexpected for grafted layers that have thicknesses between 1 and 4 nm. A too high magnitude of the contact area may partly be due to an overestimation of the stiffness k_v [Eq. (5)]. But to get reasonable values of the contact area requires to divide the announced stiffnesses by a factor of 5. Not only is such a discrepancy on the stiffness values not reasonable, but this will also mean that the same correcting factor should have to be applied for the four different cantilevers. Also, the pull-off force measurements give an overestimation similar to that obtained with the friction data. In spite of the very stable behavior and the coherent picture we get, there are still a few questions remaining to perform a complete quantitative analysis with an AFM.

With a stress activation volume $\phi = 5 \text{ nm}^3$, the interface shear strengths decrease by a factor of 25. The AFM results give shear strengths τ ranging between 8 and 11 MPa, which is exactly the domain of shear strength measured at the macroscopic scale. Moreover, the barrier heights calculated, which are independent of the activation volume chosen, are also nearly identical to the ones obtained by Briscoe and Evans.

Therefore, using the same phenomenological model to interpret the AFM results leads to quantitative values identical to that obtained at a much larger scale. In other words, the process that characterizes the dissipation of energy is independent of the scale at which the force of the friction of self-assembled or grafted layers is investigated.

This conclusion should not be so surprising. AFM deals with the concept of single asperity, which obviously comes from the size of the nanotip, but when a sliding experiment at the macroscopic scale involves soft materials on a smooth surface, there is no particular reason to consider a multiasperity problem.

This has been unambiguously shown by Grosch.^{17,18} By sliding a rubber on a glass, Grosch has been able to extract a characteristic length of 6 nm, while when using a rough surface, the characteristic length is 10^{-2} cm, corresponding to the average distance between the asperities. This experimental results clearly show that if soft materials are investigated, macroscopic sliding experiments can access molecular quantities.

Also, through an analysis of the relaxation of the frictional force, recent experiments made with a SFA apparatus show that a characteristic length of 4.5 nm was systematically observed.³⁶

If we put these results together, we might see that the stress activation volume computed by Briscoe and Evans,

and used in the present work, falls in the range of this characteristic length. It seems that as soon as ideas of viscous flow can be applied to explain the friction behavior, we end with very similar results whatever the scale at which the sliding experiment is performed and whatever the friction apparatus used.

V. CONCLUSION

The frictional forces between grafted layers on silica and a nanotip have been measured with an AFM. The change of the frictional force as a function of the tip velocity has been investigated, providing a comparative study between the friction behavior of triethoxysilane molecules grafted on the silica and polymer grafted on the triethoxysilane molecules acting as coupling agents.

For the two types of grafted layers, the forces of friction increase linearly with the logarithm of the tip velocity. The general trend of the data is correctly described with a simple stress-modified, thermally activated model. With the help of the Eyring model we compute the interface shear strengths and the barrier heights. The nanotip experiences a much higher frictional force on the polymer layer, and we systematically compute a corresponding interface shear strength twice as high as the one computed for the silane layers. Also, the barrier heights increase 30–40%. The good robustness of the behavior, observed whatever the tip used, and the use of the model make that we obtain a coherent picture from which we deduce the way the polymer has been grafted on the triethoxysilane molecules. The monomer unit has been chosen such that the polymer backbone can be grafted in several locations. The friction data sustain this possibility. We end with the conclusion that the increase of the interface shear strength and the effective barrier is due to the polymer that chemically links the organosilanes, thus increasing the number of molecules involved in the process of dissipation.

Using the stress activation volume computed by Briscoe and Evans,¹⁵ we obtained shear strengths and barrier heights for the silane layers which are remarkably closed to the ones they measured. Therefore, from the macroscopic scale down to the nanometer scale, it does appear that we can get the same behavior with very similar quantities characterizing the interface during a sliding experiment.

As the sliding friction is described with a thermally activated process, to get further quantitative insight into the friction behavior requires measurement as a function of the temperature. The present analysis suggests a liquidlike structure of the layers, and following the dynamic phase diagram,¹⁴ one can expect to reach the amorphous, more rigid state, by cooling down the sample. From a practical point of view, it can be of importance to access the different structures of the underlying coupling agent layer in order to optimize either a grafting or a polymerization process of a polymer. Such a study of the influence of the temperature is currently underway.

*Author to whom correspondence should be addressed. Fax: 33556846970. Electronic address: aime@maxime.cristal.u-bordeaux.fr

¹*Fundamentals of Friction*, Vol. 220 of NATO Advanced Study

Institute Series E: Applied Sciences, edited by I. L. Singer and H. M. Pollock (Plenum, New York, 1992).

²I. L. Singer, *J. Vac. Sci. Technol. B* **12**, 2605 (1994).

³R. M. Overney, E. Meyer, J. Frommer, D. Brodbeck, R. Lüthi, L.

- Howald, H. J. Güntherodt, M. Fujihira, H. Takano, and Y. Gotoh, *Nature (London)* **359**, 133 (1994); R. M. Overney and E. Meyer, *MRS Bull.*, 26 (May 1993).
- ⁴M. Radmacher, R. W. Tillman, M. Fritz, and H. E. Gaub, *Science* **257**, 1900 (1992).
- ⁵C. D. Frisbie, F. F. Rozsnyai, A. Noy, M. S. Wrighton, and C. M. Lieber, *Science* **265**, 2071 (1994).
- ⁶J. L. Wilbur, H. A. Biebeck, J. C. MacDonald, and G. M. Whitesides, *Langmuir* **11**, 825 (1995).
- ⁷S. Gauthier, J. P. Aimé, T. Bouhacina, A. J. Attias, and B. Desbat, *Langmuir* **12**, 5126 (1996).
- ⁸V. V. Tsukruk, V. N. Blinzyuk, D. Visser, J. Hazel, *Tribology Letters* **2**, 71 (1996); V. V. Tsukruk, V. N. Blinzyuk, D. Visser, and J. Hazel, *Langmuir* **12**, 4840 (1996).
- ⁹L. Landau and E. Lifchitz, *Theory of Elasticity* (Mir, Moscow, 1967).
- ¹⁰K. L. Johnson, K. Kendall, and A. D. Roberts, *Proc. R. Soc. London, Ser. A* **324**, 301 (1971); K. Kendall, *Nature (London)* **319**, 203 (1986).
- ¹¹D. J. Maugis, *J. Colloid Interface Sci.* **150**, 243 (1992).
- ¹²R. W. Carpick, N. Agrait, D. F. Ogletree, and M. Salmeron, *J. Vac. Sci. Technol. B* **14**, 1289 (1996).
- ¹³C. A. J. Putman, M. Igarashi, and R. Kaneko, *Appl. Phys. Lett.* **66**, 3221 (1995).
- ¹⁴H. Yoshizawa, Y. L. Chen, and J. N. Israelachvili, *J. Phys. Chem.* **97**, 4128 (1993).
- ¹⁵B. J. Briscoe and D. C. Evans, *Proc. R. Soc. London, Ser. A* **380**, 389 (1982).
- ¹⁶K. G. McLaren and D. Tabor, *Nature (London)* **197**, 856 (1963).
- ¹⁷K. A. Grosch, *Nature (London)* **197**, 858 (1963); *Proc. R. Soc. London, Ser. A* **274**, 21 (1963).
- ¹⁸J. D. Ferry, *Viscoelastic Properties of Polymers* (Wiley, New York, 1970).
- ¹⁹I. Fujiwara, T. Kamei, and J. E. Seto, *Jpn. J. Appl. Phys., Part 1* **34**, 4932 (1995).
- ²⁰Z. Elkaakour, J. P. Aimé, T. Bouhacina, C. Odin, and T. Masuda, *Phys. Rev. Lett.* **73**, 3231 (1994).
- ²¹H. J. Eyring, *J. Chem. Phys.* **3**, 107 (1937).
- ²²J. N. Glosli and G. M. McClelland, *Phys. Rev. Lett.* **70**, 1960 (1993).
- ²³Digital Instrument (Santa Barbara), V-shape AFM cantilevers (nanoprobes).
- ²⁴J. P. Aimé, in *Conjugated Polymers*, edited by J. L. Brédas and R. Silbey (Kluwer Academic, Dordrecht, 1991), pp. 229–314.
- ²⁵N. Ono, H. Miyake, T. Saito, and A. Kaji, *Synthesis* **1980**, 952; S. Gauthier, Ph.D. thesis, Université Bordeaux I, 1996.
- ²⁶J. Perez, *Physique et Mécanique des Polymères Amorphes* (Ed. Tec-Doc, Paris, 1991).
- ²⁷F. Heslot, T. Baumberger, B. Perrin, B. Caroli, and C. Caroli, *Phys. Rev. E* **49**, 4973 (1994).
- ²⁸R. J. Warmack, X. Y. Zheng, T. Thundat, and D. P. Allison, *Rev. Sci. Instrum.* **65**, 394 (1994).
- ²⁹J. P. Aimé, Z. Elkaakour, S. Gauthier, D. Michel, T. Bouhacina, and J. Curély, *Surf. Sci.* **329**, 149 (1995).
- ³⁰J. P. Cleveland, S. Manne, D. Bocek, and P. K. Hansma, *Rev. Sci. Instrum.* **64**, 403 (1993).
- ³¹J. P. Aimé, Z. Elkaakour, C. Odin, T. Bouhacina, D. Michel, J. Curély, and A. Dautant, *J. Appl. Phys.* **76**, 754 (1994).
- ³²D. Sarid, *Scanning Force Microscopy* (Oxford University Press, New York, 1991).
- ³³J. N. Israelachvili, *Intermolecular and Surface Forces* (Academic, London, 1985).
- ³⁴E. Meyer, R. Overney, D. Brodbeck, L. Howald, R. Lüthi, J. Frommer, and H.-J. Güntherodt, *Phys. Rev. Lett.* **69**, 1777 (1992).
- ³⁵C. Odin, J. P. Aimé, Z. Elkaakour, and T. Bouhacina, *Surf. Sci.* **317**, 321 (1994).
- ³⁶J. M. Georges, A. Tonck, and D. Mazuyer, *Wear* **175**, 59 (1994); (unpublished).